Structures 81 (2025) 110358

Contents lists available at ScienceDirect

Structures

journal homepage: www.elsevier.com/locate/structures

Parametric optimization of the shape of trapezoidal sheets due to the moment of inertia or covering width

T. Szumigała [a], T. Gajewski [b], T. Garbowski [c,*]

[a] *Institute of Building Engineering, Poznan University of Technology, Piotrowo 5, Poznan 60-965, Poland*
[b] *Institute of Structural Analysis, Poznan University of Technology, Piotrowo 5, Poznan 60-965, Poland*
[c] *Department of Biosystems Engineering, Poznan University of Life Sciences, Wojska Polskiego 50, Poznan 60-627, Poland*

A R T I C L E I N F O

Keywords:
Trapezoidal steel sheets
Parametric optimization
Moment of inertia
Cover width
Sequential quadratic programming (SQP)
Eurocode 3

A B S T R A C T

The study presented in this article focuses on the parametric optimization of trapezoidal steel sheets used in construction, aiming to enhance their structural efficiency and reduce material usage. The optimization addresses two primary criteria: maximizing the moment of inertia and maximizing the cover width of the sheets. The research employs the Sequential Quadratic Programming (SQP) method for optimization, considering the constraints and standards proposed in Eurocode 3. The study explores the design variables, including the dimensions of the web and flange sections, to achieve optimal geometries for both criteria. The results indicate that optimizing for the moment of inertia leads to designs with larger stiffeners and more vertical web sections, enhancing the sheet's resistance to bending. Conversely, optimizing for cover width results in designs with more delicate stiffeners and less steep web sections, increasing the sheet's surface area coverage. Both optimization approaches demonstrate significant improvements over traditional designs, showcasing potential material savings and reduced environmental impact. The findings highlight the importance of optimization in structural engineering, suggesting that tailored designs can meet specific performance requirements while adhering to practical manufacturing constraints. This research contributes to the development of more efficient and sustainable construction materials, promoting advancements in the construction industry.

1. Introduction

During designing building structures, it is necessary to take into account the safety of their users and to ensure that designed object can be used in accordance with its intended purpose. The structure should meet the conditions of limit states — ultimate and serviceability. Therefore, the task of the structural designer is to select solutions that will prevent the loads from causing the destruction of all or part of the building, or from resulting in unacceptably large displacements and deformations of the structure. The requirements of the modern world make it necessary to choose a solution that is not only safe, but also the best possible one in regard to sustainable development, material consumption and cost, taking into account various aspects.

Construction industry is perceived as high labor intensity, resource-intensive branch, having significant impact on the environment. It was reported that the construction industry was responsible for about 20 % of the total energy consumption. For instance, in China, it was reported that, the construction industry is second-largest energy consuming sector [1]. Construction contributes to carbon dioxide (CO_2) emissions on an impressive scale, accounting for as much as 30 % of global emissions of this gas [2]. Steel production is known for being one of the industrial sectors that generates the highest greenhouse gas emissions and requires large amounts of energy. The metallurgy process often relies on traditional technologies that are both energy-intensive and high-emitting. Additionally, the extraction of raw materials and transport to metallurgical plants also contribute to increasing the carbon footprint of this process.

Moreover, economic aspects are still important. The challenge is to reconcile the interests of all interested parties — the manufacturer of the product (materials), investor, designer, contractor and the user of the facility. It is obvious that each of them pays attention to different factors. The investor's goal is to obtain a building that is safe and meets functional requirements at the lowest possible costs. In turn, the designer has a huge responsibility. Not only must he develop a technical design of the

* Corresponding author.
E-mail addresses: tomasz.szumigala@put.poznan.pl (T. Szumigała), tomasz.gajewski@put.poznan.pl (T. Gajewski), tomasz.garbowski@up.poznan.pl (T. Garbowski).

https://doi.org/10.1016/j.istruc.2025.110358
Received 15 October 2024; Received in revised form 28 September 2025; Accepted 30 September 2025

object that will be functional, safe and economical, but also compliant with a number of regulations. Ideally, the contractor's abilities, experiences and resources should be taken into account. This would avoid designing solutions that may be difficult to implement or require unattainable resources. From the contractor's point of view, solutions that are less time-consuming and do not require much work and resources are beneficial. In terms of cold formed structures, price is a serious concern. The cost of cold rolled steel is twice as much as the cost of hot rolled steel [3]. Lower demand for materials reduces the investor's costs. Lighter elements make the assembly process easier for the contractor. The accessibility of effective solutions enhances the efficiency of structural design.

Therefore, in a world where sustainability, energy efficiency and economics are key priorities, the construction industry faces a challenge: how to achieve excellence in the design, construction and operation of buildings, while ensuring optimal use of resources/materials and minimal environmental impact. In this context, attention should be paid to trapezoidal sheets, very popular material, widely used for roof and wall coverings. Optimizing their cross-section will decrease demand for steel and bring a reduction in the carbon footprint, energy consumption and costs.

There are three generations of trapezoidal sheets: first – walls of the cross-section has no stiffeners, second – longitudinal stiffeners are used and the third generation – both longitudinally and transversely stiffened sheets are utilized. First generation trapezoidal sheet are used in lower spans, to about 3.5 m, in which the loads are relatively small, their height of cross-section is approximately up to 70 mm. Second and third generation sheets are often used in roofs without purlins. In such situation, trapezoidal sheet is supported directly by the upper chord of the girder. If appropriate, the connection between sheet and the supporting element ensures that the trapezoidal sheet can function as lateral restraint, preventing the upper chord from buckling [4,5]. Providing sufficient flexural stiffness of the sheet and torsional stiffness of the connection between cladding and upper chord can result in limiting lateral deformations also in lower chord [6]. However, replacing bracing with trapezoidal sheets requires caution both in the design and assembly process [7]. Second generation sheets are used when spacing of supports is up to 10 m. Third generation trapezoidal sheets are often used in concrete-steel composite structures and with support spacing up to 15 m.

Trapezoidal sheets are thin-walled elements, which means they are classified as class four cross-sections. In such situation, a reduced cross-section is used to calculate the geometric parameters due to the loss of local stability of the slender walls. The procedure for determining the effective cross-section is time-consuming, therefore, in practice, the designers select the cross-section of trapezoidal sheets based on the manufacturer's tables. This means that the knowledge of procedure of determining the effective cross-section of trapezoidal sheets is not common among engineers and no optimisation analyses are conducted. Ajdukiewicz and Gajewski [8] identified form of buckling of thin-walled element under compression using deformations theorem and finite element method (FEM). Flat and curved trapezoidal sheets were also analysed using yield line theory [9].

This study primarily emphasizes the presentation of an algorithm for determining the optimal design of a specific type of steel trapezoidal sheet in accordance with Eurocode standards. The investigation focuses on the outcomes of constrained optimization applied to 135 mm sheets, specifically addressing: (a) the maximization of moment of inertia, and (b) the maximization of cover width. These results are thoroughly examined and discussed within the context of the study.

In literature, the majority of analyses concerning optimal design focus on single criterion scalar optimization, where the most common criterion is weight of the structure [10,11]. However, the benefits of this approach in practical tasks are limited. More efficient method used in the structure optimization is multi-criteria optimization. Bicriteria optimization for thin-walled beams was presented in [12–15]. For instance, in [15], an optimization analysis for simply supported thin-walled beams subjected to pure bending was performed. The optimization criterion were the area of the cross-section and deflection, which depends on cross-section stiffness, therefore on the moment of inertia. Complex parametric analyses were performed for beams with perforation [16]. Also, in terms of trapezoidal sheets, in [17], optimization using genetic algorithms was performed for cross-sections of low height and without intermediate stiffeners. In [18], an objective measure of the effectiveness of existing high cross-sections with transversal stiffeners was found by introducing an original coefficient depending on the width of the covering, the strength index and the cross-sectional area. In scientific literature, there is a lack of studies on the optimal selection of cross-section of the trapezoidal sheet. Therefore, in this study, efforts were made to find a cross-section of trapezoidal sheet that could be more efficient than those currently available on the market in regard to (i) the maximization of moment of inertia, and (ii) the maximization of the cover width.

2. Methods and materials

2.1. Stated optimization problem

The aim of this study is to find optimal designs for trapezoidal sheets. In task (i), the optimal geometry is sought concerning the maximum moment of inertia, I, assuming a minimum cover width, $B_{\min}$, fixed metal sheet width, L, and the height of the trapezoidal sheet, H. In task (ii), the optimal geometry is sought concerning the maximum cover width of a single trapezoidal sheet, B, assuming a minimum initial value of moment of inertia, $I_{\min}$, fixed metal sheet width, L, and the height of the trapezoidal sheet, H.

The optimization problem is stated as finding the maximum moment of inertia as follows:

$$I(\boldsymbol{x}) = \sum_{i=1}^{n} \left(I_i(\boldsymbol{x}) + A_i(\boldsymbol{x}) e(\boldsymbol{x})_i^2\right),\ \boldsymbol{x} \in X \tag{1}$$

In which $I_i(\boldsymbol{x})$ is the local moment of inertia of single element, while $A_i(\boldsymbol{x})$ is the area of the single element and $e(\boldsymbol{x})$ is the offset from the centroid of element to the neutral axis of the entire trapezoidal profile.

On the other hand, the form of the objective function regarding the maximum cover width reads:

$$B(\boldsymbol{x}) = 6\cdot(\mathrm{w_{s1}} + \mathrm{w_{s2}} + \mathrm{w_{s3}} + \mathrm{w_{s3}} + \mathrm{w_{s2}} + \mathrm{ws1}) + 3\cdot\left(\mathrm{w_{p2}} + \mathrm{w_{p1}} + \mathrm{w_{p2}} + \mathrm{w_{p1}} + \mathrm{w_{p2}}\right) + 3\cdot\mathrm{w_{p3}},\ \boldsymbol{x} \in X \tag{2}$$

Please refer to Fig. 1 and Table 1 for a description of the optimization

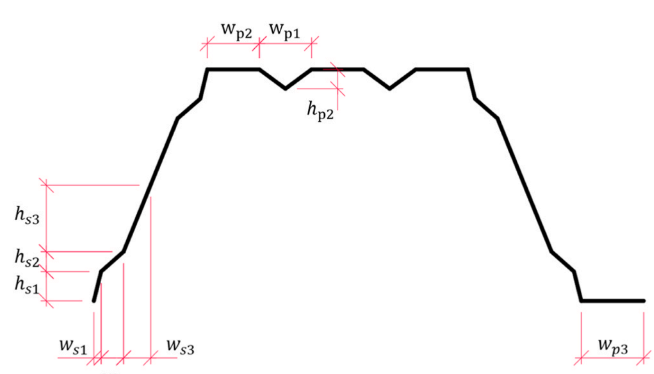

Fig. 1. Design variables considered in the optimization analysis for the trapezoidal sheets, explained in Table 1 (with the exception of right side element, w_{p3}, the geometry is symmetrical).

Table 1
The lower limits, upper limits and initial values of design parameters assumed in the optimization analyses.

Symbol	Description	Lower limit $b_{\min}$	Upper limit $b_{\max}$	Initial
h_{s1} (mm)	height of the first section of the web	10	20	16.2
h_{s2} (mm)	height of the stiffener of the web	1	15	13.4
h_{s3} (mm)	height of the second section of the web	30	40	37.3
w_{s1} (mm)	width of the first section of the web	1	15	5.95
w_{s2} (mm)	width of the stiffener of the web	1	15	11.6
w_{s3} (mm)	width of the second section of the web	10	30	16.7
h_{p1} (mm)	height of the stiffener of the flange	5	10	6.5
w_{p1} (mm)	width of the stiffener of the flange	10	40	30.1
w_{p2} (mm)	width of the sections of the flange	10	40	27.3
w_{p3} (mm)	width of the bottom flange	20	40	39.3

symbols.

All optimization analyses were conducted for trapezoidal sheets with a height of 135 mm, metal sheet width of 1500 mm and sheet thickness of 1 mm. The optimization analyses focused on symmetric sheets with 2 stiffeners in the web and 2 stiffeners on the flanges.

Design variables, $\boldsymbol{x}$, included the height and width of the web sections, the height and width of the flange sections, and the width of the sheeting lock. Design variables considered are presented in Fig. 1, with symbols explained in Table 1. It should be noted, that with the exception of far right-hand side element (w_{p3}), the analysed system is symmetrical. The table also presents the lower and upper limits of design parameters. The adopted limits result from a review of existing commercial trapezoidal sheet solutions in the European market. Also, the following constraints were assumed for (i) optimization regarding maximum moment of inertia:

$$L(\boldsymbol{x}) \leq 1500mm, \tag{3}$$

$$H(\boldsymbol{x}) \leq 135mm, \tag{4}$$

$$B(\boldsymbol{x}) \geq 955mm, \tag{5}$$

in which, L is the metal sheet width, H is the height of the trapezoidal profile and B is cover width of the trapezoidal profile.

In (ii) optimization, regarding the maximum cover width, similar constraints were assumed:

$$L(\boldsymbol{x}) \leq 1500mm, \tag{6}$$

$$H(\boldsymbol{x}) \leq 135mm, \tag{7}$$

$$I(\boldsymbol{x}) \geq 94910 \quad mm^4, \tag{8}$$

in which, L is the metal sheet width, H is the height of the trapezoidal profile and I is the intertia moment of the trapezoidal profile.

The Eqs. 3 and 6 represent the maximum sheet width resulting from the specifications of production machines. Obviously, sheets with higher heights will achieve much better performance. Hence, conditions in Eqs. 4 and 7 assume limitation to one type of trapezoidal sheet. Since maximizing, I and B are in contradiction, conditions in Eqs. 5 and 8 enforce finding a structures that will be not only optimal for particular criteria (I for (i) optimization or B for (ii) optimization), but also practical from the application point of view – i.e. the new values for optimal design will be no worse than for the initial design case. $B = 955mm$ and $I = 94910mm^4$ are the values obtained for initial design case, see the last column of Table 1.

Initial values of design parameters in optimization analyses are presented in Table 1. They were determined based on trapezoidal sheet cross-sections available on the market. Furthermore, technological and practical constraints were also taken into account. For example, width of the bottom flange should provide space for placing connectors. Also, if the sheet is intended for assembly in the negative position, this limitation applies to the top flange. In terms of maximal dimensions, to large widths of the walls of the cross-section cause significant reduction of the effective width due to higher slenderness. Therefore, some of the dimensions were constrained to avoid exploring unreasonable areas of the optimization space.

In this scientific work, the Sequential Quadratic Programming (SQP) method was used as the mathematical optimization method, which has proven its effectiveness in many studies [16,19]. A significant advantage of SQP method is that, with a relatively small number of function evaluations, it allows finding an optimal solution. Although it is susceptible to finding local minima, preliminary investigations have shown that the adopted objective functions are not multimodal. The optimization method used is described in Subsection 2.2.

Optimally designed load-bearing trapezoidal sheets are thin-walled structures; hence, it is necessary to consider local stability loss when calculating their load-bearing capacity. In the computational algorithm used in this work, local stability loss was taken into account based on the approach from Eurocode 3 [20]. Details of the employed method are presented in Subsection 2.3.

2.2. Optimization method

In this study, the sequential quadratic programming (SQP) method was used for the purpose of finding optimal design of trapezoidal sheets. Its reliability was shown on benchmark examples available in [21–25]. Moreover, the method proved its effectiveness in a multiple scientific studies by solving engineering problems, for instance in optimal design of concrete bubble deck slabs [19].

SQP represents the nonlinear programming methods, in which:

$$F(\boldsymbol{x}) \quad , \tag{9}$$

is subjected to nonlinear constraints, i.e.,:

$$C(\boldsymbol{x}) \leq 0,$$

$$\boldsymbol{A} \bullet \boldsymbol{x} \leq \boldsymbol{b},$$

$$\boldsymbol{b}_{\min} \leq \boldsymbol{x} \leq \boldsymbol{b}_{\max}, \tag{10}$$

$F(\boldsymbol{x})$ is the cost function of the design parameters, $\boldsymbol{x}$. $\boldsymbol{b}$ and $\boldsymbol{b}_{eq}$ are one-column matrices. $\boldsymbol{A}$ and $\boldsymbol{A}_{eq}$ are matrices; C and C_{eq} are functions. $\boldsymbol{b}_{\min}$ and $\boldsymbol{b}_{\max}$ represent the lower and upper boundaries of the design parameters. Equality constraints also are possible by the following:

$$C_{eq}(\boldsymbol{x}) = 0,$$

$$\boldsymbol{A}_{eq} \bullet \boldsymbol{x} = \boldsymbol{b}_{eq}, \tag{11}$$

The constraints are considered by solving the Lagrangian subproblem:

$$L(\boldsymbol{x}, \lambda) = F(\boldsymbol{x}) + \sum_{i=1}^{m} \lambda_i \bullet g(\boldsymbol{x}), \tag{12}$$

here, λ_i are the Lagrange multipliers, while $g(\boldsymbol{x})$ represents the constraints.

To linearize the nonlinear constraints the sequential quadratic subproblem is obtained by the following:

$$\frac{1}{2}\boldsymbol{d}^T\boldsymbol{H}_k + \nabla F(\boldsymbol{x}_k)^T\boldsymbol{d}$$

$$\nabla g_i(\boldsymbol{x}_k)^T\boldsymbol{d}+g_i(\boldsymbol{x}_k)=0$$

$$\nabla g_i(\boldsymbol{x}_k)^T\boldsymbol{d}+g_i(\boldsymbol{x}_k)\leq 0 \tag{13}$$

H_k is the approximation of the Hessian matrix. The approximation of the Hessian matrix is computed according to the Broyden-–Fletcher–Goldfarb–Shanno (BFGS) method [26–29].

The new solution is obtained iteratively:

$$\boldsymbol{x}_{k+1}=\boldsymbol{x}_k+\alpha_k\boldsymbol{d}_k \tag{14}$$

α_k is a step length parameter.

2.3. Designing of trapezoidal metal sheet according to Eurocode 3

The great slenderness of the walls of the cross-section of trapezoidal sheet causes their vulnerability to local and distortional buckling [30]. Local buckling is related to the loss of stability of the central surface of the wall of a thin-walled element without changing the position of the corners of the cross-section. The distortion is revealed by displacement of corners caused by buckling of adjacent walls. On the other hand, in case of general buckling, all corners of the cross-section change their position. The influence of local and distortion instability is taken into account in calculation of the load capacity by limiting the geometric characteristics of the gross cross-section to the geometric characteristics of the equivalent cross-section. It is provided by reducing the actual width of the walls to the effective widths.

2.3.1. Thickness and thickness tolerances

Thickness and its tolerances given in the standard [20] may be used for steel within the following ranges of the core thickness (t_{cor}) in terms of sheeting and members: 0.45 mm - 15 mm. It is permissible to use thicker or thinner material. In such situation, the bearing resistance has to be confirmed by tests. The design thickness denoted by t depends on the core thickness and minus tolerance. For tolerance less than or equal to 5 %, the design thickness is equal to the core thickness. The core thickness is equal to the nominal thickness t_{nom} decreased by the metallic coating thickness, which is assumed to be 0.04 mm for zinc coating.

2.3.2. Geometrical proportions

The regulations given in the standard [20] cannot be applied for cross-sections outside the range width-to-thickness ratio shown in the Table 5.1 of the standard. If the properties of the effective cross-section are confirmed by testing and calculations, those limits can be ignored.

2.3.3. Influence of rounded corners

Rounded corners of cross-sections complicate the calculation of geometric and strength characteristics. In order to facilitate the calculation of those characteristics, the standard regulations allow for the simplification of the cross-section geometry by eliminating rounded corners from the cross-section and leaving flat walls with the conventional width. Rounded corners can be neglected if the internal radius is less or equal five times design thickness and less or equal 0.10 b_p (notional flat width).

2.3.4. Determination of geometric characteristic of the effective cross-section

The effective widths of unstiffened elements should be obtained from [20]. Width of the wall is assumed as notional flat width b_p. The reduction factors for plate buckling are obtained basing on the plate slenderness $\bar{\lambda}_p$.

2.3.5. Trapezoidal sheeting profiles with intermediate stiffeners

The procedure of determining geometrical characteristics of the effective cross-section of the flange will be presented in the forthcoming sections.

Firstly, the effective widths $b_{1,e1}$ and $b_{1,e2}$, of the wall in the case of one stiffener and $b_{1,e2}$ and $b_{2,e1}$ respectively, in the case of two stiffeners must be determined. One must carry out the calculations as for flat walls without stiffeners and assuming that the flat parts are supported on both sides.

Secondly, for the cross-section of the effective stiffener (or stiffeners) determined in previous step, the critical elastic stress $\sigma_{cr,s}$ depending on the number of stiffeners should be computed. For one central flange stiffener, the elastic critical buckling stress is obtained from:

$$\sigma_{cr,s}=\frac{4.2\quad k_wE}{A_s}\sqrt{\frac{I_st^3}{4{b_p}^2(2b_p+3b_s)}}\quad, \tag{15}$$

in which b_s is the width of the stiffener, E is Young modulus, A_s and I_s are geometrical characteristics of the stiffener and k_w is a coefficient that allows for partial rotational restraint of the stiffened flange by the webs or other adjacent elements.

Thirdly, if the webs of the trapezoidal sheet are unstiffened, based on the elastic critical stress $\sigma_{cr,s}$ determined in the second step, the relative slenderness $\bar{\lambda}_d$ according to formula 5.12d of the standard must be calculated. If the web of the trapezoidal sheet is also stiffened, the relative slenderness is calculated based on the modified $\sigma_{cr,\mathrm{mod}}$ value.

In the fourth step, depending on the relative slenderness obtained in the third step, the reduction factor χ_d due to distortion buckling (flexural buckling of the stiffener) according to formulas 5.12a to 5.12c of the standard are computed. For the coefficient χ_d determined in the previous step, the effective cross-section of the stiffener with reduced thickness t_{red} according to 5.5.3.4.2(11) of the standard are determined. Above mentioned formulas, the formulas 5.12a to 5.12c are taking into account the impact of the slenderness of the element:

$$\chi_d=1 if\bar{\lambda}_d\leq 0.65, \tag{16}$$

$$\chi_d=1.47-0.723\bar{\lambda}_d if 0.65<\bar{\lambda}_d<1.38, \tag{17}$$

$$\chi_d=\frac{0.66}{\bar{\lambda}_d} if\bar{\lambda}_d\geq 1.38 \tag{18}$$

The relative slenderness is obtained using the following relation:

$$\bar{\lambda}_d=\sqrt{\frac{f_{yb}}{\sigma_{cr,s}}}\quad, \tag{19}$$

where f_{yb} is basic yield strength.

The determination of effective widths of the web with intermediate stiffeners will be presented in the forthcoming paragraphs. Firstly, one must determine the initial location of the neutral axis of the section composed of the effective sections of the flange and the gross sections of the web. Secondly, the effective widths from $s_{eff,0}$ to $s_{eff,n}$ according to formulas (5.32) to (5.33 f) of the standard depending on the number of stiffeners must be computed:

$$s_{eff,0}=0.76t\sqrt{E/(\gamma_{M0}\sigma_{com,Ed})}, \tag{20}$$

where $\sigma_{com,Ed}$ is the stress in the flange under compression when the cross-section resistance is reached;

$$s_{eff,1}=s_{eff,0}, \tag{21}$$

$$s_{eff,2}=(1+0.5h_a/e_c)s_{eff,0,} \tag{22}$$

$$s_{eff,3}=[1+\frac{0.5(h_a+h_{sa})}{e_c}]s_{eff,0,} \tag{23}$$

$$s_{eff,4}=(1+0.5h_b/e_c)s_{eff,0}, \tag{24}$$

$$s_{eff,5} = \left[1 + \frac{0.5(h_b + h_{sb})}{e_c}\right] s_{eff,0}, \quad (25)$$

in which e_c is the distance from the effective centroidal axis to the system line of the flange under compression; h_a, h_b, h_{sa} and h_{sb} are dimensions connected with the part of the web under compression.

Thirdly, basing on the widths obtained in the second step one must verify whether the flat widths are fully effective. If not, calculated effective widths remain unchanged. If the conditions are met the effective widths are revised using formulas from 5.34a to 5.38b of the standard depending on the number of stiffeners in the web:

- for unstiffened web, if $s_{eff,1} + s_{eff,n} \geq s_n$, the entire web is effective, so the widths are revised in the following way:

$$s_{eff,1} = 0.4 s_n \quad (26)$$

$$s_{eff,n} = 0.6 s_n \quad (27)$$

for stiffened web, if $s_{eff,1} + s_{eff,2} \geq s_a$, the whole length of s_a is effective, so the revision is as follows:

$$s_{eff,1} = \frac{s_a}{2 + 0.5 h_a / e_c} \quad (28)$$

$$s_{eff,2} = s_a \frac{1 + 0.5 h_a / e_c}{2 + 0.5 h_a / e_c} \quad (29)$$

for web with one stiffener, if $s_{eff,3} + s_{eff,n} \geq s_n$, the whole length of s_n is effective, therefore, the widths are revised in the following way:

$$s_{eff,3} = s_n \frac{1 + 0.5(h_a + h_{sa})/e_c}{2.5 + 0.5(h_a + h_{sa})/e_c} \quad (30)$$

$$s_{eff,n} = s_n \frac{1.5 s_n}{2.5 + 0.5(h_a + h_{sa})/e_c} \quad (31)$$

for web with two stiffeners:

o if $s_{eff,3} + s_{eff,4} \geq s_b$, the whole length of s_b is effective, so the revision is as follows:

$$s_{eff,3} = s_b \frac{1 + 0.5(h_a + h_{sa})/e_c}{2 + 0.5(h_a + h_{sa} + h_b)/e_c} \quad (32)$$

$$s_{eff,4} = s_b \frac{1 + 0.5 h_b / e_c}{2 + 0.5(h_a + h_{sa} + h_b)/e_c} \quad (33)$$

if $s_{eff,5} + s_{eff,n} \geq s_n$, the whole length of s_n is effective, so the widths are revised in the following way:

$$s_{eff,5} = s_b \frac{1 + 0.5(h_b + h_{sb})/e_c}{2.5 + 0.5(h_b + h_{sb})/e_c} \quad (34)$$

$$s_{eff,n} = s_b \frac{1.5 s_n}{2.5 + 0.5(h_b + h_{sb})/e_c} \quad (35)$$

Then, the elastic critical buckling stress $\sigma_{cr,sa}$ for the web stiffener is determined:

$$\sigma_{cr,sa} = \frac{1.05 k_f E \sqrt{I_s t^3 s_t}}{A_{sa} s_2 (s_1 - s_2)} \quad (36)$$

where s_1 is obtained in the following way:

- for a single stiffener:

$$s_1 = 0.9(s_a + s_{sa} + s_c) \quad (37)$$

for the stiffener closer to the flange under compression, in webs with two stiffeners:

$$s_1 = s_a + s_{sa} + s_b + 0.5(s_{sb} + s_c) \quad (38)$$

$$s_2 = s_1 - s_a - 0.5 s_{sa} \quad (39)$$

while k_f is a coefficient that allows for partial rotational restraint of the stiffened web by the flanges. Conservatively, it may be taken as equal to 1 what corresponds to a pin-jointed condition. I_s is the second moment of area of a stiffener cross-section consisting of the fold width s_{sa} and two adjacent strips, each of width $s_{eff,1}$, about its own centroidal axis parallel to the plane web elements.

If the flanges are unstiffened, the reduction factor χ_d is obtained directly from $\sigma_{cr,sa}$. If the flanges are also stiffened, the reduction factor χ_d should be obtained using the method basing on the modified elastic critical stress $\sigma_{cr,\mathrm{mod}}$:

$$\sigma_{cr,\mathrm{mod}} = \frac{\sigma_{cr,s}}{\sqrt[4]{1 + \left[\beta_s \frac{\sigma_{cr,s}}{\sigma_{cr,sa}}\right]^4}} \quad , \quad (40)$$

in which $\beta_s = 1$ for a profile in axial compression, while $\beta_s = 1 - (h_a + 0.5 h_{sa})/e_c$ for a profile under bending.

This enables obtaining relative slenderness. Next, basing on the value of the relative slenderness, the reduction factor is determined. Then, the reduced effective area of the stiffener $A_{sa,red}$ is calculated using the reduced thickness:

$$t_{red} = \chi_d t. \quad (41)$$

$$A_{sa,red} = \frac{\chi_d A_{sa}}{1 - (h_a + 0.5 h_{sa})/e_c} \mathrm{but} A_{sa,red} \leq A_{sa}. \quad (42)$$

The effective section properties can be refined iteratively by assuming the location of the effective centroidal axis basing on the effective cross-sections determined in the previous iteration. This iteration should be based on an increased basic effective width $s_{eff,0}$.

3. Results

3.1. Optimization with respect to moment of inertia

In the optimization study, two types of cost function criteria were used. In this subchapter, the results from maximising the moment of inertia assuming the minimal cover width were presented. In Fig. 2, the results are presented for iterations of minimization algorithm. In Fig. 2a, the convergence of the design parameters is shown. For more details about the design parameters, please refer to Fig. 1 and Table 1. In Fig. 2b, the maximization of the moment of inertia (cost function, blue plot) and corresponding strength index (red plot) were demonstrated. The strength index was computed using the classic formula, i.e., by dividing the moment of inertia by the maximum coordinate with respect to the neutral axis of the cross-section. In Fig. 2c, the change of metal sheet width is plot, as the consequences of changing design parameters. Dashed line represents the upper limit set in the optimization, resulting from production capabilities.

In Table 2, the final optimal designs are shown. In the second column of the table, the optimal design parameters of trapezoidal sheet with respect to moment of inertia are shown. Moreover, the initial design geometry as well as the optimal design determined are demonstrated in Fig. 3a,b, respectively.

3.2. Optimization with respect to sheet cover width

In this subchapter, the results from maximising the sheet cover width assuming the minimal moment of inertia are presented. In Fig. 4, the results are showed for iterations of minimization algorithm. In Fig. 4a, the convergence of the design parameters is shown. For more details

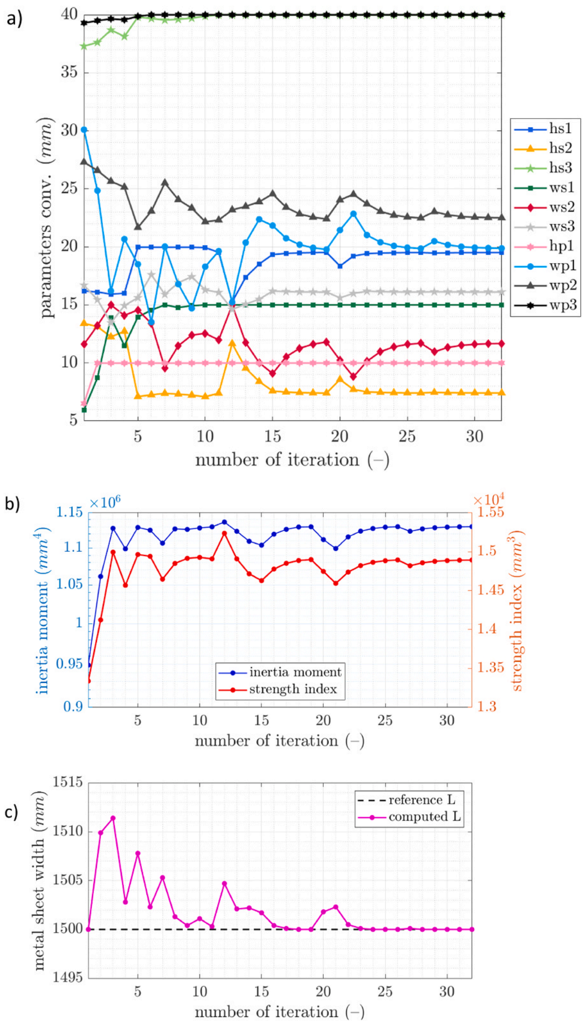

Fig. 2. Deriving optimal design of trapezoidal sheet with respect to moment of inertia: (a) design parameters convergence, (b) increasing moment of inertia as cost function maximization and (c) respecting the limitations of metal sheet width (1500 mm limit).

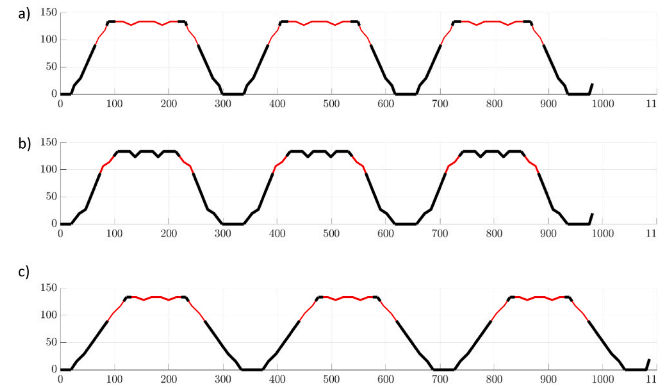

Fig. 3. Trapezoidal sheet cross-sections: (a) initial design for starting optimization, (b) optimal design in respect to moment of inertia and (c) optimal design in respect to cover width.

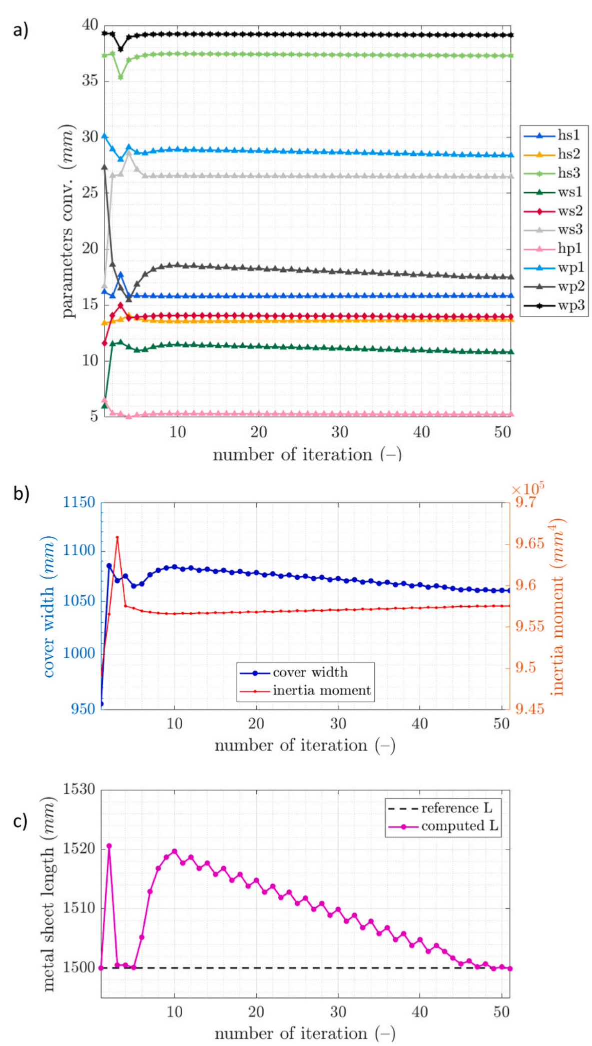

Fig. 4. Deriving optimal design of trapezoidal sheet with respect to sheet cover width: (a) design parameters convergence, (b) increasing moment of inertia as cost function maximization, and (c) respecting the limitations of metal sheet width.

Table 2
The initial and optimal design parameters in optimization in respect to: (i) moment of inertia and (ii) sheet cover width.

Physical quantity	Optimal solution in respect to moment of inertia, *I*	Optimal solution in respect to sheet cover width, *B*
h_{s1} (mm)	19.5	15.8
*hs*2 (mm)	7.4	13.7
h_{s3} (mm)	40.0	37.3
w_{s1} (mm)	15.0	10.8
w_{s2} (mm)	11.7	14.0
w_{s3} (mm)	16.1	26.5
h_{p1} (mm)	10.0	5.2
w_{p1} (mm)	20.0	28.4
w_{p2} (mm)	22.4	17.5
w_{p3} (mm)	40.0	39.1
I (mm^4)	1,130,130 (119.1 %)	957,560 (100.9 %)
B (mm)	955.2 (100.0 %)	1 060.5 (111.0 %)

about the design parameters, please refer to Fig. 1 and Table 1. In Fig. 4b, the maximization of the sheet cover width (cost function, blue plot) and corresponding inertia moment (red plot) are demonstrated.

In Fig. 4c, the change of metal sheet width is plot as the consequences of changing design parameters. Dashed line represents the upper limit set in the optimization, resulting from production capabilities.

As previously, the final optimal design is shown in Table 2. In the third column of the table, the optimal design parameters of trapezoidal sheet with respect to sheet cover width are demonstrated. Furthermore, for comparison, the initial design geometry as well as the optimal design achieved is presented in Fig. 3a,c, respectively.

4. Discussion

In the optimization study, two types of cost function criteria were considered. Both analysis gave different results, what was shown in Fig. 3. The multicriteria approach was not employed in the paper because it always requires assigning weight factors, which in our opinion would be subjective. In addition, the focus of the paper is on achieving better results relative to the initial case, which was actually a commercial profile, while still preserving its key characteristics from an industrial point of view.

In Fig. 3, inn the optimization in respect to moment of inertia, the design parameters demonstrated much higher fluctuations throughout the optimization process, please see Fig. 2a. Updating the parameters is more rapid, two types of parameter trends may be observed. Namely, h_{s3}, w_{s1}, h_{p1} and w_{p3}, after a few iterations achieves its upper boundaries, thus, their maximization to elevate the moment of inertia seems to be unequivocal. Other parameters fluctuate; the highest activity in comparison to its initial values may be observed for h_{s2} and w_{p1}. It is worth noting that h_{s3} is maximized from the beginning with minor fluctuation in favour of h_{s1} and h_{s2}. h_{s1} and h_{s2} determines the stiffening in the corner, thus, its length cannot be directly maximized, since it would cause local instability and therefore exclusion or weakening of the contribution of this part of the cross-section when calculating the moment of inertia.

The activity of the parameters has its reflection in the cost function (CF), please see Fig. 2b. Rapid increase in the CF is caused by maximization of h_{s3}, w_{s1}, h_{p1} and w_{p3} (3rd iteration), simultaneously, the limitation in metal sheet width is violated, please see Fig. 2c. Further, the optimization algorithm seeks for solution that is not violating the constraints. The violation is successively decreased with preserving high values of moment of inertia. In 12th iteration, the algorithm substantially changes selected parameters (h_{s1}, h_{s2}, w_{s2} and w_{p1}), what has some reflection in CF, but it is more significant in metal sheet width. Similar behaviours may be observed in iterations 15 and for 19 – 21 for similar sets of parameters (for 15th iteration w_{s2}, w_{p1} and w_{p2}, and for 19th – 21st iterations w_{p2} h_{s2}, w_{s2}, w_{p1} and w_{p2}), here, smaller sheet width constraint violations were noticed. Slight effect may be also observed in 27th iteration, however, with not so significant effects in parameters, CF or metal sheet width. To sum up, the biggest activity is noticed and the careful decision while optimal design in respect to moment of inertia must be taken for h_{s1}, h_{s2}, w_{s2} w_{p1} and w_{p2}, i.e., for web: height of the first section, height of the stiffener, width of the stiffener and for flange: width of the stiffener and width of the sections, respectively.

The moment of inertia of the optimal design of trapezoidal sheet increased up to 1,130,130 mm^4, which was 119.1 % of the initial value; the cover width, B, was the same as the initial design, and the metal sheet width of 1500 mm was also achieved, see the second column in Table 2.

In the optimization process concerning the width of the sheet cover, the design parameters demonstrated significant changes up to approximately 6th iteration, after which their alterations became more gradual throughout the optimization process, please see Fig. 4a. Here, updating the values of selected parameters (w_{s1}, w_{p1} and w_{p2}) up to the last iteration was slow and stable —comparing to the optimization process in respect to moment of inertia. Obviously, w_{p1} and w_{p2} were crucial, because they directly determines the cover width, B. w_{s1} role was important because it influences the stiffening of the corner and thus may cause potential local instability of the web. Other parameters hold their values from approximately 10th iteration, namely, h_{s1}, h_{s2}, h_{s3}, w_{s2}, w_{s3}, h_{p1} and w_{p3}. Such behaviour has its reflection in cost function criteria and corresponding moment of inertia.

Up to 6th iteration, the cover width increases rapidly, above 1 060 mm, see Fig. 4b, however, with violating the constraint of metal sheet width due to production (1500 mm), see Fig. 4c. Later, in the optimization process, the algorithm gradually reduces the cost function value while simultaneously decreasing the violation of the metal sheet width constraint to finally achieve non-violation for relatively high cover width. The positive effect was the gradual increase of the moment of inertia.

The cover width of the optimal design of trapezoidal sheet increased up to 1 060.5 mm, which was 111.0 % of the initial value; the moment of inertia, I, was slightly bigger than for the initial design (100.9 %), and the metal sheet width of 1500 mm was also achieved, see the third column in Table 2.

The comparison of the geometry of the initial design and the optimal designs makes it possible to draw general conclusions regarding optimal structures depending on the adopted criterion, see Fig. 3. The optimal design in regard to the moment of inertia has larger stiffeners in the flange with no cross-sectional exclusion, a more vertical web and larger sheet bending angles, both in the web and in the flange. The optimal structure in regard to the cover width has delicate stiffeners and a less steep web; also, bending angles are much smaller.

5. Conclusions

In the study, the optimization of trapezoidal sheets was conducted by parametrically determining the shape of the cross-section using the method presented in Eurocode 3. This method involves limiting the geometric features of the gross cross-sections to those of an equivalent section by reducing the actual width of the walls to effective widths, and segmentally reducing the walls thickness. The optimization presented independently sought the best solutions for: (i) maximum moment of inertia given a minimum required cover width, and (ii) maximum cover width while maintaining the effective moment of inertia of the cross-section.

The study demonstrated that the use of optimization algorithms allows to find solutions that improved the trapezoidal sheet performance, depending on the criterion considered, compared to a reference commercial solution. The results show that manufacturers adopt solutions with relatively large material reserves and that it is possible to reduce the cross-section without deteriorating other properties of the trapezoidal sheet.

CRediT authorship contribution statement

Tomasz Szumigała: Writing – review & editing, Writing – original draft, Visualization, Validation, Investigation, Formal analysis. **Tomasz Garbowski:** Writing – review & editing, Supervision, Software, Project administration, Methodology, Conceptualization. **Tomasz Gajewski:** Writing – review & editing, Writing – original draft, Visualization, Validation, Software, Methodology, Investigation, Formal analysis.

Declaration of Competing Interest

The authors declare that they have no known competing financial interests or personal relationships that could have appeared to influence the work reported in this paper.

References

[1] Xu G, Wang W. China's energy consumption in construction and building sectors: an outlook to 2100. Energy 2020;195:117045.
[2] Tan X, Lai H, Gu B, Zeng Y, Li H. Carbon emission and abatement potential outlook in China's building sector through 2050. Energy Pol 2018;118:429e39.
[3] Billah M, Islam Md M, Bin Ali R. Cold formed steel structure: an overview. An International Scientific Journal, 118. WSN; 2019. p. 59–73. EISSN 2392-2192.

[4] Biegus A, Czepiżak D. Corrugated sheet as a bracing of flat truss chords their out-plane buckling. ISSN 0137-2971 MaterłY Bud 2015;(nr 514). https://doi.org/10.15199/33.2015.06.01.
[5] Gryniewicz M., Szlendak J.K., FEM model of the steel building roof includes stressed skin diaphragm action effects, doi: 10.1201/b21417-12.
[6] Gozzi J. Design of roof trusses. AccessSteel SN027a-EN-EU. 2006. ⟨www.steel-access.com⟩.
[7] Niewiadomski L., Słowiński M., Błędy projektowe i wykonawcze konstrukcji przekrycia hali stalowej, Nowoczesne hale 3/11.
[8] Ajdukiewicz C., Gajewski M., Identyfikacja formy utraty stateczności sprężystego ściskanego pręta cienkościennego przy wykorzystaniu MES i teorii dużych deformacji.
[9] Casariego P, Casafont M, Ferrer M, Marimon F. Analytical study of flat and curved trapezoidal cold formed steel sheets by means of the yield line theory. Part 1: flat sheets without transverse corrugations. Thin Walled Struct 2019;141:675–92. https://doi.org/10.1016/j.tws.2018.12.017.
[10] Tian YS, Lu TJ. Minimum weight of cold-formed steel sections under compression. Thin Walled Struct 2004;42:515–32.
[11] Seaburg PA, Salmon CG. Minimum weight design of light gage steel members. J Struct Div 1971;97:203–22.
[12] Ostwald M, Rodak M. Multicriteria optimization of cold-formed thin-walled beams with generalized open shape under different loads. Thin Walled Structures65 2013: 26–33.
[13] Kasperska R., Magnucki K., Ostwald M., Bicriteria optimization of cold-formed thin-walled beams with open cross-sections, Proceedings of WCSM06 2005, 29 May-5 June Rio de Janeiro, Brazil.
[14] Magnucki K, Ostwald M. Optimal design of selected open cross sections of cold-formed thin-walled beams. Pozn Pozn Univ Technol Publ 2005.
[15] Ostwald M, Rodak M. Bicriteria optimization problem of cold-formed thin-walled beams with selected open cross section. In: Zingoni A, editor. Recent developments in structural engineering, mechanics and computation. Rotterdam: Millpress; 2007.
[16] Gajewski T, Staszak N, Garbowski T. Parametric optimization of Thin-Walled 3D beams with perforation based on homogenization and soft computing. Materials 2022;15:2520. https://doi.org/10.3390/ma15072520.
[17] Mezzomo GP, Iturrioz I, Grigoletti G, Gomes HM. Influence of the fixing type in the optimization of trapezoidal roofing sheets. J Constr Steel Res 2014;96:26–39.
[18] Rzeszut K, Szumigała T. Optimal design methods of trapezoidal steel sheets. AIP Conf Proc 2019;2060:020011. https://doi.org/10.1063/1.5086142.
[19] Gajewski T, Staszak N, Garbowski T. Optimal design of bubble deck concrete slabs: serviceability limit state. Materials 2023;16:4897. https://doi.org/10.3390/ma16144897.
[20] PN-EN 1993-1-3: Eurocode 3 - Design of steel structures - Part 1-3: General rules - Supplementary rules for cold-formed members and sheeting.
[21] Biggs MC. Constrained minimization using recursive quadratic programming. Towards Global Optimization. The Netherlands: North-Holland: Amsterdam; 1975.
[22] Han SP. A globally convergent method for nonlinear programming. J Optim Theory Appl 1977;22:297–309. https://doi.org/10.1007/bf00932858.
[23] Powell MJD. The convergence of variable metric methods for nonlinearly constrained optimization calculations. Proceedings of the Special Interest Group on Mathematical Programming Symposium Conducted by the Computer Sciences Department at the University of Wisconsin–Madison, July 11–13. MA, USA: Academic Press: Cambridge; 1977. https://doi.org/10.1016/b978-0-12-468660-1.50007-4.
[24] Powell MJD. A fast algorithm for nonlinearly constrained optimization calculations. Numer Anal 1978;630:144–57.
[25] Nocedal J, Wright SJ. Numerical optimization. Springer Series in Operations Research. 2nd ed. Berlin/Heidelberg, Germany: Springer; 2006.
[26] Broyden CG. The convergence of a class of Double-rank minimization algorithms 1. General considerations. IMA J Appl Math 1970;6(1):76–90. https://doi.org/10.1093/imamat/6.1.76.
[27] Fletcher R. A new approach to variable metric algorithms. Comput J 1970;13(3): 317–22. https://doi.org/10.1093/comjnl/13.3.317.
[28] Goldfarb D. A family of Variable-Metric methods derived by variational means. Math Comput 1970;24(109):23–6. https://doi.org/10.2307/2004873.
[29] Shanno DF. Conditioning of Quasi-Newton methods for function minimization. Math Comput 1970;24(111):647–56. https://doi.org/10.2307/2004840.
[30] Pięciorak E., Piekarczyk M., Determination of effective cross-section for trapezoidal sheet in bending according to PN-EN 1993-1-3 Standard.